Available online at www.sciencedirect.com
SCIENCE DIRECT
International Journal of Multiphase Flow 32 (2006) 269–284
International Journal of Multiphase Flow
www.elsevier.com/locate/ijmulflow

Stepped chutes: Pre-aeration and spray reduction

Michael Pfister, Willi H. Hager *, Hans-Erwin Minor

VAW, ETH Zentrum, CH-8092 Zurich, Switzerland

Received 21 July 2005; received in revised form 19 October 2005

Abstract

Stepped chutes are a standard element in hydraulic engineering. Among others, two basic problems have not yet been addressed so far. These include the direct spray reduction on stepped chutes for relatively small discharges by an improved step edge geometry, and the cavitation damage up to the point of self-aeration for relatively large discharges. This research adds to these two items by systematic observations on a stepped chute of definite slope and step size. The test data were analyzed resulting in preliminary recommendations for an improved performance of stepped chutes. It was concluded that the present knowledge applies also for stepped chutes extended with an aerator as proposed herein. The latter may be easily added to existing designs, of which the design discharge is increased.

Keywords: Aerator; Cavitation; Chute; Spray; Stepped spillway

1. Introduction

Stepped chutes have become a standard hydraulic structure within the past decades. They are currently an alternative design to smooth spillways, with a major difference in the maximum hydraulic load (Vischer and Hager, 1998). Whereas the smooth spillway may be subjected with unit discharges of over 100 m^2/s, current design guidelines for the stepped chute propose a maximum unit discharge of less than 30 m^2/s (Pfister et al., in press, see also Appendix 1). Accordingly, stepped chutes are currently employed for relatively small discharges. In contrast, smooth chute spillways are designed for both large discharges and hydraulic heads, together with an appropriate protection against cavitation damage. Once the large cavitation damages were detected in the 1960s, means were developed to counter that self-damaging mechanism. It was realized in the 1970s that the only technical means to counter cavitation damage is the chute aerator (Pinto et al., 1982; Falvey, 1990). Volkart and Chervet (1983) were among the first to propose various designs for an adequate presence of air close to the chute bottom. Such an effort was not made until today for stepped chutes, however.

* Corresponding author. Tel.: +41 44 632 4149; fax: +41 44 632 1192.
E-mail address: hager@vaw.baug.ethz.ch (W.H. Hager).

0301-9322/$ - see front matter © 2005 Elsevier Ltd. All rights reserved.
doi:10.1016/j.ijmultiphaseflow.2005.10.004

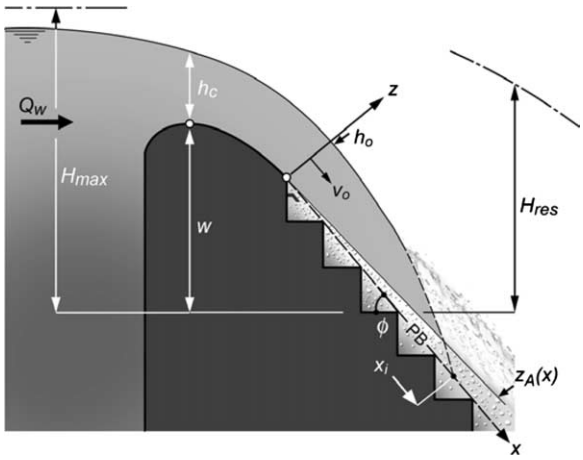

Fig. 1. Definition sketch for pre-aerated stepped chute flow, PB = pseudo-bottom.

A second problem so far not systematically investigated is the stepped chute performance for small discharges. Depending on the chute slope and the step height, spray production develops for discharges below a certain limit discharge (Mateos Iguácel and García, 2000; Chamani, 2000). The resulting flow does then no more attach to the chute bottom, but is deflected towards the air to impact further downstream onto a step edge. Due to the steep impact angle, the flow is again deflected away from the stepped chute and produces a significant amount of spray. Spray is a nuisance in hydraulic engineering for various reasons: (1) erosion of adjacent embankments made of sediment; (2) spray generation and ice production in cold regions; (3) loss of a significant amount of the discharge during heavy wind, and (4) requirement of a higher freeboard.

The following relates to both, the pre-aeration of stepped chute flow for large discharges and the reduction of spray for relatively small discharges. The research is preliminary in the sense that only one stepped chute was available, with a fixed step height and a constant angle of the pseudo-bottom (PB) (Fig. 1). However, the model employed simulates typical stepped chute flow, given that the angle of the pseudo-bottom was 50°, and the model step height was with almost 0.10 m relatively large. The analysis of data was generalized to provide results that are directly applicable for the chute geometry investigated. More research is needed to expand the results for a generalized hydraulic approach. It should be noted that both the Reynolds and the Weber number were sufficiently high to allow for the Froude similitude in discussing the main features of the air–water flow (Boes and Hager, 2003a).

2. Hydraulic model

The experiments were conducted in the VAW stepped chute model. The angle of the pseudo-bottom $\phi = 50°$ (1V:0.84H) is commonly used for stepped chutes in dam engineering. The water (subscript w) discharge Q_w overflows a standard crest geometry whose design (subscript D) head was $H_D = 0.524$ m. For a chute width of $B = 0.500$ m, the crest design discharge is $Q_D = 0.432$ m^3/s therefore, corresponding to almost 1 m^3/s per unit width of the model chute. The step height of the model was $s = 0.093$ m; a total of 25 steps were provided along the chute length of 3.03 m. If a prototype step height of 1.20 m (4 ft) would be considered, the model scale is 1:12.9, and it would increase to 1:3.2 for a prototype step height of 0.30 m (1 ft). This large model was particularly built to counter effects of scale, therefore. The instrumentation employed for the present research was an updated RBI twin fiber-optical probe extensively described by Boes (2000). The free surface of the flow was investigated using digital photography rather than a conventional point gage because of the spray formation. The water discharge was recorded to ±3% using inductive discharge measurement (IDM). The air discharge was not directly measured because of the relatively complicated model air supply system, as described below.

3. Pre-aerated chute flow

3.1. Definitions

Fig. 1 shows a scheme of the model used. A water discharge Q_w overtopped the crest with the critical flow depth $h_c = [Q_w^2/(gB^2)]^{1/3}$, with g as the acceleration of gravity. A coordinate system (x, z) with x as the streamwise coordinate and z vertical on it was placed at the beginning of the first step. At the section $x = 0$, the average flow depth is h_o and the average velocity is v_o. A so-called *step aerator* to be described below was inserted in the first step to aerate the bottom portion of the stepped chute. Accordingly, the flow is white close to the steps up to the aeration (subscript A) height $z_A(x)$. At the free surface, a blackwater flow extends up to the point of surface air inception, along with an expansion of the surface air entrainment towards the stepped chute bottom, as for the conventional stepped chute. The incipient (subscript i) bottom aeration sets in at location x_i downstream from the first step (Fig. 1). At a certain elevation w from the spillway crest, the residual (subscript res) energy head of the air–water mixture flow is H_{res}, with $H_{res} < H_{max}$ due to the energy dissipation.

The experimental program involved three discharges, namely $Q_w/Q_D = 0.10$, 0.26 and 0.56. The lower discharge was the minimum under which no appreciable spray formation resulted, whereas the large discharge was the maximum under which air by the present aerator was still entrained. As discussed below, the upper limit of air entrainment is related to a minimum local Froude number and the particular aerator design adopted herein. Table 1 summarizes the main flow characteristics investigated with column 1 as the run number. Columns 2–4 relate to the critical flow depth h_c, the flow depth h_o upstream of step 1 and the water discharge per unit width q_w, q_A is the air discharge per unit width, x_i is the incipient bottom air entrainment point if the aerator would be absent, and h_{wu} is the uniform (subscript u) blackwater flow depth. Further, C_{au} is the uniform average (subscript a) air concentration in the uniform flow reach with h_{90u} as the uniform air–water mixture flow depth, C_{bu} is the bottom (subscript b) air concentration for uniform flow and $\beta = q_A/q_w$ is the ratio between the air and water discharges. Numbers in *italic* were predicted from Boes (2000) and Boes and Hager (2003a,b), whereas the remainder was measured on the model. Because of the limited chute length, the uniform flow parameters could only be observed for the smaller discharges.

The data relative to the spray formation are sensitive to scale effects. With the relatively large hydraulic model employed in the present study these should be relatively small, however. The limit Reynolds and Weber numbers as proposed by Boes (2000) were exceeded, except for the smallest discharge investigated. The effect of spray in hydraulic engineering poses problems that cannot be definitely accounted for until today, and the results should be considered with attention, therefore.

3.2. Novel step aerator

Problems with cavitation damage in smooth spillways were successfully countered with chute aerators. Three main aerator types were proposed (Volkart and Chervet, 1983): (1) deflector corresponding to a wedge on a straight bottom, (2) drop as an elevation difference between the upstream and downstream bottom profile, and (3) groove with an aerator placed at the upstream groove side. The latter type is hardly used because of the risk of choking air supply, whereas both types (1) and (2) are extensively applied in hydraulic engineering, in addition to combinations of the two.

Table 1
Test data for step aerator

Run	h_c [m]	h_o [m]	q_w [m^2/s]	q_A [l/s m]	x_i [m]	h_{wu} [m]	C_{au} [–]	C_{bu} [–]	h_{90u} [m]	β [%]
a	0.090	0.028	0.084	1.767	0.243	0.022	0.559	0.262	0.050	2.10
b	0.173	0.071	0.226	0.865	0.877	*0.043*	*0.582*	*0.251*	*0.102*	0.38
c	0.289	0.132	0.487	0.520	*2.506*	*0.070*	*0.562*	*0.232*	*0.161*	0.11

Values in *italic* according to Boes (2000) and Boes and Hager (2003a).

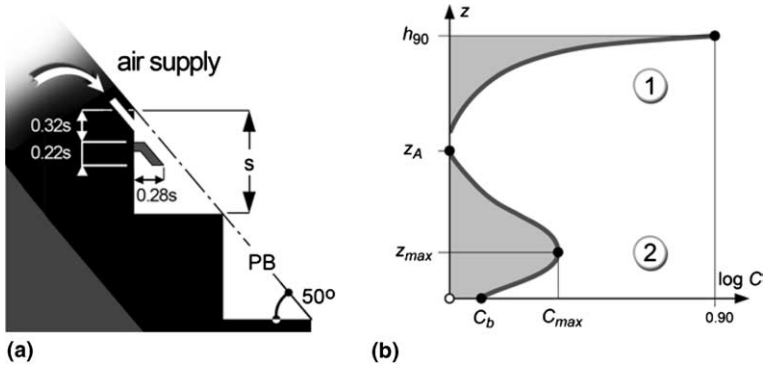

Fig. 2. Definition sketches: (a) aerator employed in present research, (b) twin aeration profile by ① free surface entrainment and ② pre-aeration at pseudo-bottom.

A logic approach for stepped chutes was therefore to insert a deflector type aerator upstream of the first step (Pfister et al., in press). However, a deflector lifts the flow slightly above the pseudo-bottom resulting in flow impact onto the steps. No particular disadvantages may be observed for larger discharges except for the flow deflection at the impact location, and an appreciable loss of air from the aerated chute flow because of jet compression in the vicinity of the jet impact. For smaller discharges, a significant spray is produced because of jet impact onto the horizontal step faces.

Whereas the bottom pressure along a smooth straight spillway is practically hydrostatic, stepped chutes develop strong vorticity in the step niches. It is known from detailed pressure readings (Sánchez Juny et al., 2000) that the pressure on the horizontal step face is more than hydrostatic because of jet impact, whereas the pressure along the vertical step face decreases from the step corner towards the step edge. Accordingly, the vertical face downstream of the step edge is a zone of relative small pressure favorable for an aerator. Fig. 2(a) shows the novel 'step aerator' proposed for stepped chutes. It essentially consists of a 2D lip extending across the chute with a horizontal portion close to the vertical step face, and a sloping portion close to the pseudo-bottom (PB), of which the angle was equal to ϕ. A much larger hydraulic model would be required for a detailed appreciation of the optimum aerator design. This was outside from the research objective, however.

The principle of the novel 'step aerator' is as follows: The step niche is subdivided into a positive pressure zone below the aerator lip due to the jet impact, and a negative pressure zone above the aerator lip. Without this separation element—herein referred to as the aerator—the subpressure required to supply air to the flow is too small according to preliminary tests. As indicated in Fig. 1, an air boundary layer develops upstream from the first step edge. The exact amount of air supply is subject to detailed future research. It is notable that the particular aerator used herein entrained an adequate amount of air by the high-speed flow for the discharges listed in Table 1. Further, the air diffusion in the z-direction was relatively small resulting in a concentrated air–water layer close to the steps. The particular advantages of the step aerator are: (1) concentrated air supply at the first step, (2) aerator may be added to existing designs, (3) air addition to step niches resulting in cavitation protection of stepped chute, and (4) moderate bottom air entrainment along the chute with a small increase of the flow depth. The following discusses the main two-phase flow features along the stepped chute for a pre-aerated flow.

3.3. Bottom air concentration

Fig. 3(a)–(c) shows the air concentration distributions $C(z/h_{90})$ at various sections downstream from $x = 0$. A semi-logarithmic plot was selected to appreciate the features of the air–water flow. The typical development of air entrainment is explained in Fig. 1: The origin $(x;z) = (0;0)$ may be regarded as a point source from where the air diffuses both into the oncoming flow and transversally into the step niches. Each profile is characterized by the point of maximum air concentration $(C_{max};z_{max})$ and the height of air–water flow $z_A(x)$, as

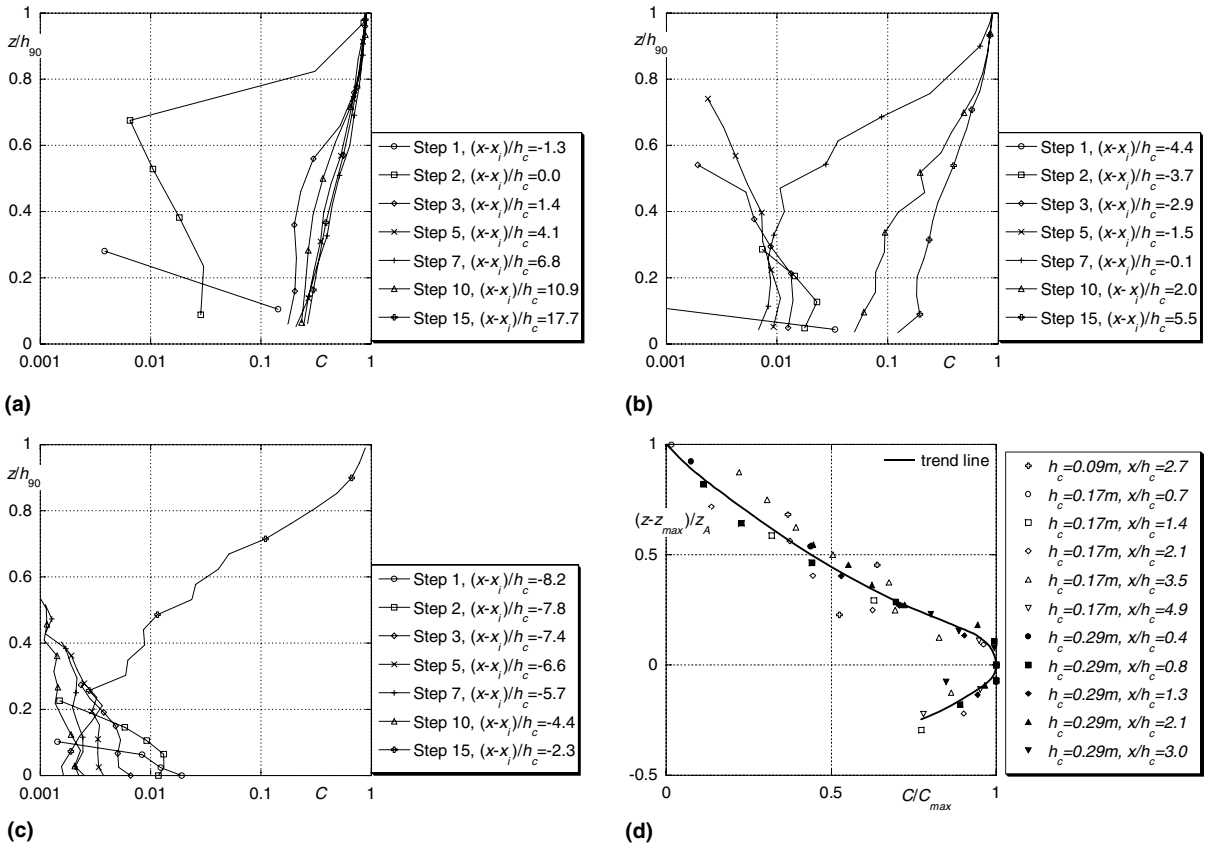

Fig. 3. Air concentration distributions $C(z/h_{90})$ at various sections $(x - x_i)/h_c$ and step number for h_c [m] = (a) 0.090, (b) 0.173, and (c) 0.289; (d) summary plot of pre-aeration profiles.

shown in Fig. 2(b). The air from the free surface may be considered as a second point source of which the origin is $x > 0$. The latter reaches the pseudo-bottom for case (a) at step 3, for (b) at step 7 and for (c) at step 15 (Fig. 3(a)–(c)).

The transverse distribution of the air concentration originating from the step aerator was further considered in Fig. 3(d): Using the coordinates C/C_{max} for relative air concentration where C_{max} is described below, and $(z - z_{max})/z_A$ allows plotting a generalized curve that resembles the velocity distribution of a plane wall jet. Accordingly, one might refer for the lower portion to as the viscous layer, and to as the diffusion layer for the upper layer.

Fig. 4 relates the scalings previously introduced to the basic hydraulic parameters of the aerator design adopted. Fig. 4(a) shows the maximum cross-sectional air concentration C_{max} relative to the air supply β versus the relative distance x/h_c with correlation coefficient $R^2 = 0.96$ as

$$\frac{C_{max}}{\beta} = 7.5 \cdot \left(\frac{x}{h_c}\right)^{-1}, \quad \text{for } 0.5 < x/h_c < 5.0 \tag{1}$$

For a given β, the maximum air concentration reduces linearly from the origin, therefore. Fig. 4(b) shows the local increase of the ratio z_{max}/h_c with x/h_c, resulting with $R^2 = 0.98$ in

$$\frac{z_{max}}{h_c} = 0.035 \cdot \frac{x}{h_c} - 0.009, \quad \text{for } 0.3 < x/h_c < 3 \tag{2}$$

The transverse height of the air–water flow above the pseudo-bottom is $z_A(x)$, where $z_A = z(C = 0)$ according to Fig. 2(b). Fig. 4(c) shows the function scaled with the critical flow depth h_c. The data follow a tangent hyperbolic function with $R^2 = 0.97$ as

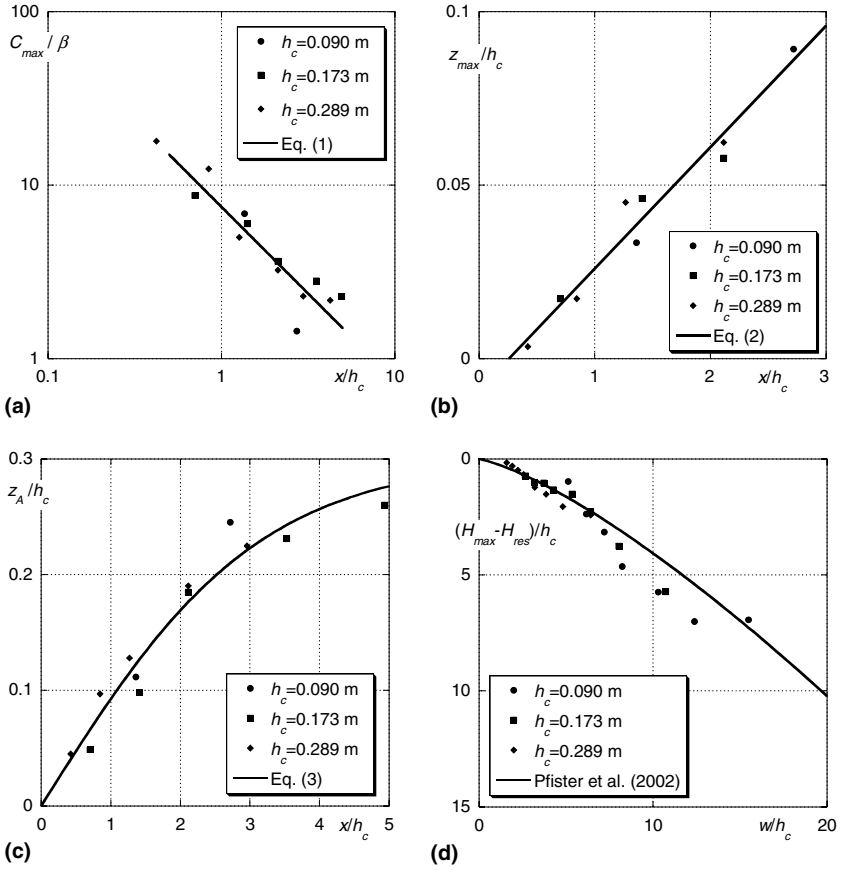

Fig. 4. Characteristics of bottom aeration: (a) relative maximum air concentration C_{max}/β with (—) (1), (b) relative elevation z_{max}/h_c with (—) (2), (c) thickness of bottom aeration z_A/h_c with (—) (3), all as a function of dimensionless distance x/h_c, (d) residual energy head $(H_{max} - H_{res})/h_c$ along stepped chute for un-aerated and pre-aerated flows.

$$\frac{z_A}{h_c} = 0.3 \cdot \tanh\left(\frac{x}{3h_c}\right), \quad \text{for } 0 < x/h_c < 5 \tag{3}$$

The thickness $z_A(x)$ of the air–water layer above the pseudo-bottom increases linearly close to the origin, and then levels off to a final value close to $z_A/h_c = 0.30$. Note that uniform aerated stepped chute flow was only reached for run (a), whereas the stepped chute was too short for the larger discharges. Using the scaling h_{90u} instead of h_c produced a poorer data correlation close to the aerator than (3).

3.4. Free surface characteristics

Fig. 5 relates to the characteristics of the free surface profile, both for blackwater and whitewater. The point of incipient air entrainment x_i without chute bottom aeration is relevant here; it was determined from Boes and Hager (2003a,b) and checked on the model. Deviations between the two approaches were typically within $\pm 1 \cdot h_c$. This was considered accurate enough for a highly turbulent flow and also demonstrated that the free surface air entrainment is not essentially influenced by pre-aeration.

Fig. 5(a) shows the dimensionless mixture free surface profile h_{90}/h_{90u} as a function of $(x - x_i)/h_c$ resulting in a single band for the three test discharges. Up to the minimum flow depth slightly upstream of $(x - x_i) = 0$, the mixture surface height decreases significantly, and increases further downstream to asymptotically reach the mixture uniform flow depth $h_{90}/h_{90u} = 1$. Note that $x = x_i$ relates to the point where the bottom air concentration is $C_b = 0.01$ according to Boes and Hager (2003a,b). The surface air entrainment point is located slightly upstream from $x = x_i$, therefore (Fig. 5(a)).

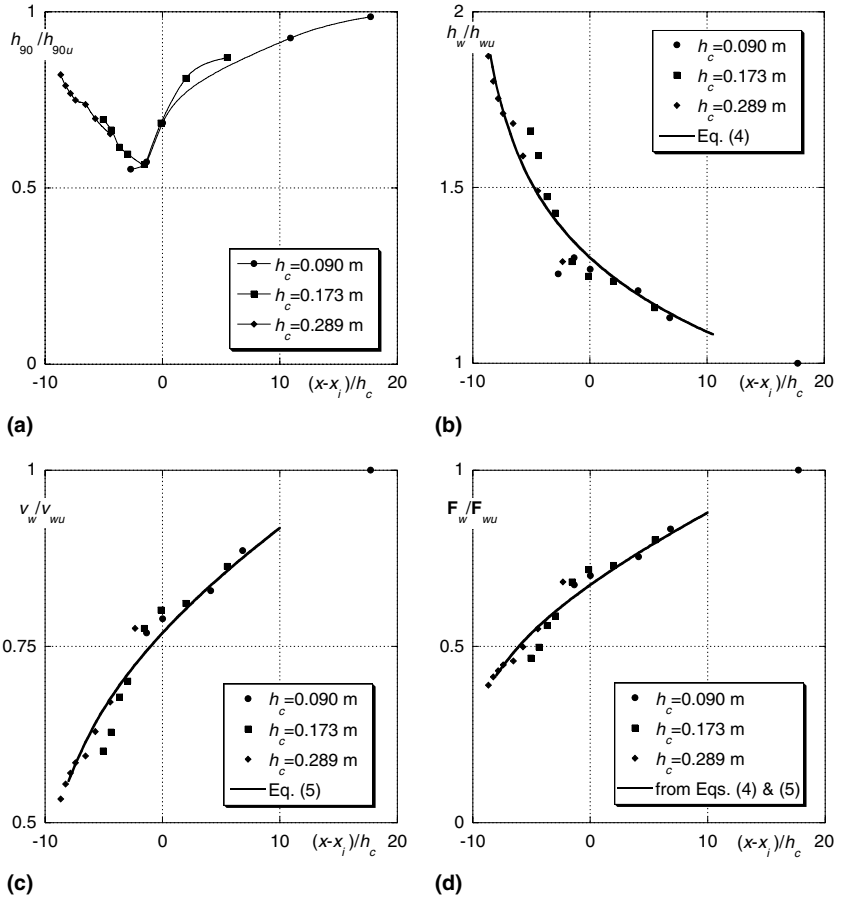

Fig. 5. Free surface characteristics: (a) whitewater flow depth h_{90}/h_{90u}, (b) blackwater flow depth h_w/h_{wu} with (—) (4), (c) average velocity development v_w/v_{wu} with (—) (5), and (d) development of Froude number F_w/F_{wu}, all as a function of dimensionless distance $(x - x_i)/h_c$.

Fig. 5(b)–(d) relate to the blackwater flow characteristics determined from the observed air concentration curves. The blackwater flow depth $h_w = (1 - C_a)h_{90}$ decreases logarithmically from the origin $x = 0$ towards the uniform blackwater flow depth h_{wu}. The data were plotted in Fig. 5(b) as h_w/h_{wu} versus $(x - x_i)/h_c$ resulting with $R^2 = 0.97$ in

$$\frac{h_w}{h_{wu}} = 2 - 0.7 \cdot \log\left[\frac{x - x_i}{h_c} + 10\right], \quad \text{for } -10 < (x - x_i)/h_c < +10 \tag{4}$$

The uniform flow was not reached with the present tests due the limited chute length. The drawdown curve (4) resembles previous observations conducted for instance by Hager and Blaser (1998). Fig. 5(c) relates to the blackwater velocity $v_w = q_w/h_w$. The data were plotted as v_w/v_{wu} versus again $(x - x_i)/h_c$. The continuity equation for blackwater flow requires $Q_w = Bh_w v_w = Bh_{wu}v_{wu}$, such that

$$\frac{v_w}{v_{wu}} = \left(\frac{h_w}{h_{wu}}\right)^{-1} \tag{5}$$

The streamwise blackwater velocity is inverse to the blackwater flow depth, therefore.

Knowing both the blackwater flow surface $h_w(x)$ and the blackwater velocity profile $v_w(x)$ allows determining the local Froude number of the blackwater flow. With $F_w = v_w/(gh_w)^{1/2}$, (4) and (5) result in $F_w = (h_w/h_{wu})^{-3/2}$. This is plotted in Fig. 5(d) showing an almost perfect agreement with the data.

3.5. Air concentration development

Fig. 6(a) shows the ratio between the average air concentration C_a and the uniform average air concentration C_{au} as a function of dimensionless location $(x - x_i)/h_c$. Despite the data scatter the three runs investigated have a similar trend. According to Boes (2000), the average air concentration at the point of bottom air inception is $C_{ai} = 0.246$ for stepped chutes without pre-aeration independent of step height and chute angle. Further, with $C_{au} = 0.57 \pm 0.01$ from Boes (2000), the ratio amounts to $C_{ai}/C_{au} = 0.43 \pm 0.01$. For the present data, similar numbers result at $(x - x_i)/h_c = 0$ (Fig. 6(a)). Therefore, this ratio seems to be independent from pre-aeration, given the relatively small air supply from the step aerator as compared to the much larger air entrainment from the free surface.

Fig. 6(b) relates the streamwise development of the bottom air concentration C_b/C_{bu} to the dimensionless location $(x - x_i)/h_c$. Note that the aerator section is located more upstream for large discharges than for small, because the streamwise origin is at $x - x_i = 0$. For the small discharge with $h_c = 0.090$ m and $C_{bu} = 0.262$, the bottom air concentration increases steeply to a first maximum of $C_{b,max}/C_{bu} = 0.55$ at $(x - x_i)/h_c = -1.3$, then decreases to $C_{b,min}/C_{bu} = 0.11$ at $(x - x_i)/h_c = 0$ and from there increases towards the uniform bottom concentration $C_{bu} = 0.262$, or $C_b/C_{bu} = 1$. For the maximum discharge with $h_c = 0.289$ m and $C_{bu} = 0.232$, the maximum relative bottom air concentration is much smaller with $C_{b,max}/C_{bu} = 0.06$ at location $(x - x_i)/h_c = -7.8$ and decreases to almost $C_b = 0$ further downstream. The stepped chute was again too short for an air supply from the free surface. For the middle discharge with $h_c = 0.173$ m an intermediate behavior

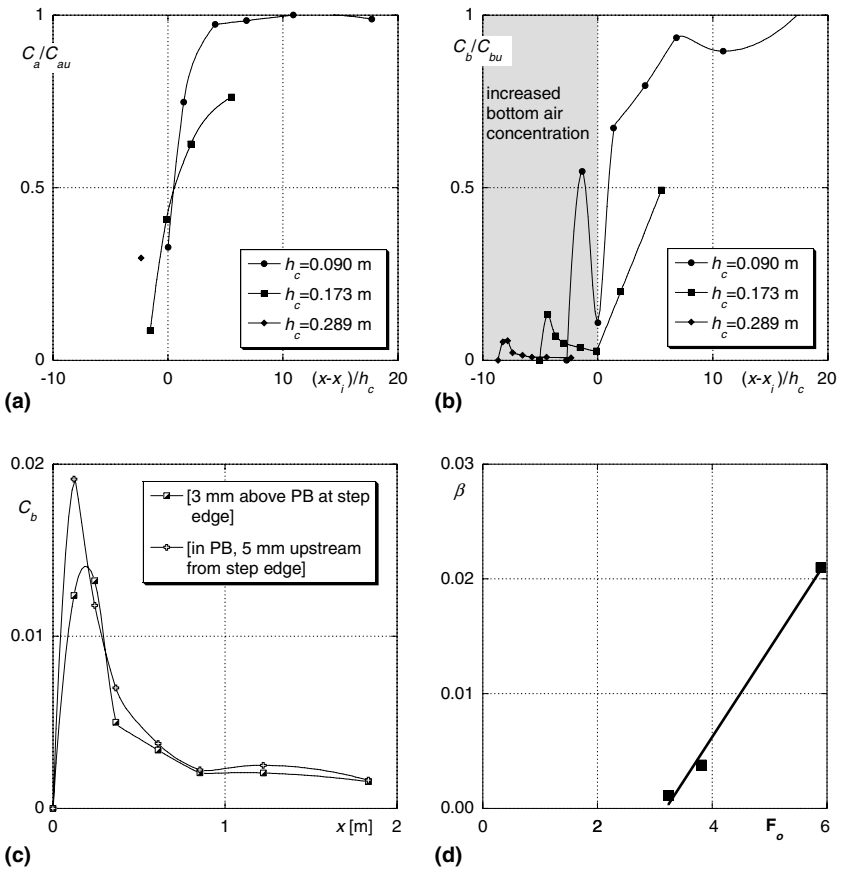

Fig. 6. Characteristics of air concentration: (a) relative average air concentration C_a/C_{au}, (b) relative bottom air concentration C_b/C_{bu} both as a function of $(x - x_i)/h_c$, (c) comparison of bottom air concentrations measured at two different, but close locations, (d) air entrainment rate β as a function of Froude number F_o in the approach flow with (—) (6).

may be observed. This plot demonstrates that much less air is entrained by the step aerator than from the free surface. The relatively small air presence close to the steps has no significant effect on the basic features of stepped chute flow which therefore apply as for chutes with an aerator.

Fig. 6(c) compares the bottom air concentration at the step edge measured 3 mm away from the pseudo-bottom with the observation 5 mm upstream from the step edge at the (virtual) elevation of the pseudo-bottom for $h_c = 0.289$ m. The two data series practically collapse except at the point of maximum bottom air concentration, where the value at pseudo-bottom elevation is larger. Herein, all observations were made exactly at the step edge section from 3 mm towards the free surface.

Fig. 6(d) gives a trend for the air supply from the step aerator employed, as a function of the Froude number $F_o = v_o/(gh_o)^{1/2}$ at the origin $x = 0$ as

$$\beta = 0.0077 \cdot (F_o - 3.2), \qquad \text{for } 3.2 < F_o < 6.0 \tag{6}$$

Compared to aerators on smooth chutes, such as those investigated by Rutschmann and Hager (1990) with an inception Froude number of 6, air entrainment for stepped chutes occurs at a significantly lower Froude number. This is an important design aspect because stepped chute flows have normally a much smaller Froude number at the aerator location than those in smooth spillways.

3.6. Energy loss

Pre-aerated stepped chute flow was also tested for the energy loss. Fig. 4(d) shows the relative energy loss $(H_{max} - H_{res})/h_c$ as a function of the relative crest elevation w/h_c (Fig. 1). The present data follow the curve previously suggested by Pfister et al. (2002). This finding again suggests that pre-aeration of a stepped chute has no essential effect on the performance of the stepped chute flow.

3.7. Photographs

The previous findings are highlighted with selected photographs to appreciate the technical results. Fig. 7 shows flows on a standard stepped chute without step aeration. It is noted that the point x_i of the bottom air inception moves continuously downstream as the discharge increases, resulting in a long distance between the spillway crest and the bottom air inception point for a large discharge. For a prototype design discharge of 100 m^2/s and $s = 1.20$ m for example, the length would be 132 m, for otherwise equal conditions as adopted herein (Boes and Hager, 2003a,b). The current maximum unit discharge for stepped chutes is of the order of 30 m^2/s. Its increase due to a reduction of the spillway width requires bottom aeration.

Fig. 8 relates to the same conditions as Fig. 7, now with pre-aeration from the first step. The air supply reduces as the water discharge increases, with air presence close to the chute bottom even for case (c) with a relatively large discharge. More importantly, the transverse air diffusion is small, such that the air remains close to the chute bottom and does practically not detrain from the flow. Fig. 8(c) demonstrates that the air is entrained into the step niches and therefore actively protects the steps from cavitation damage.

Fig. 9 shows details of the air entrainment and the air diffusion close to the aerator section. In (a) with $h_c = 0.090$ m, only the two top steps would not be protected without an aerator, because of the small discharge. However, for the large discharge in (c), an air layer extends above the steps and adds significantly to the hydraulic performance of the chute.

4. Reduction of spray

4.1. Spray formation

Spray production is a nuisance in hydraulic engineering, as outlined in Section 1. Spray was always a concern with energy dissipators, both for stilling basins and trajectory spillways. Stepped chutes are also known for the phenomenon. Mateos Iguácel and García (2000) proposed the gradual increase of step height from shortly downstream of the spillway crest to the beginning of the stepped chute for spray reduction. Their design was tested for a definite spillway resulting in an acceptable performance. However, their design involves

the step addition in a curved concrete surface over a certain length and appears to be relatively costly. An alternative proposal is made hereafter, therefore. Supercritical flow is prone to any changes of the parameters involved. Wall deflections, drops or curves result in shock waves set up usually at the downstream channel wall and extending obliquely across the tailwater chute. The first step of a stepped chute may be considered as a drop if the flow depth in the approach flow is relatively small. The jet is deflected to the vertical due to gravity and a relatively large jet portion impacts the horizontal step face. Because of the relatively small flow depth, the flow is thus deflected away from the stepped chute into the atmosphere, and the contact with the chute is lost for a number of steps. Upon re-impact on the stepped chute, the flow is re-deflected resulting in a flow that may neither be described by skimming nor by nappe flow (Ohtsu et al., 2001). From a practical point of view, such flow is unacceptable because of the large freeboard required, the small energy dissipation and the poor hydraulic performance.

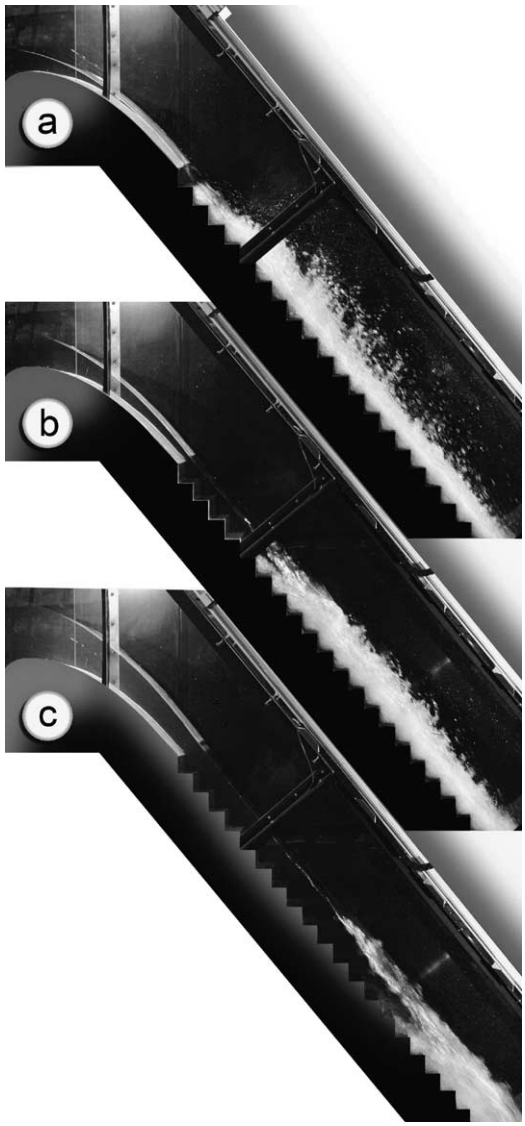

Fig. 7. Stepped chute flow *without* bottom aeration for cases (a)–(c) from Table 1.

4.2. Spray reduction

If a water jet impacts a flat plate, spray is developed. The amount of spray is large if the jet impinges almost vertically onto the plate, and reduces as the impact angle decreases. To reduce spray, the jet impact angle should be small, therefore. This concept was applied in the present research. Because the chute angle on a stepped chute is a basic design parameter, the jet impact angle was reduced by changing the step edge geometry. Instead of using a standard step with a horizontal step face, the step edge was cut close to the jet impact angle. To simplify construction, 20 mm high step insets were added to the original model steps. Fig. 10 shows flows for the specific discharge $q_w = 0.040\ m^2/s$ ($h_c = 0.055$ m) on a 50° stepped chute with (a) the standard step arrangement, (b) the first two step edges from step origin cut and (c) the first five step edges cut. It was observed that the first step edge should have an angle smaller than the pseudo-bottom, such as 40° instead of 50°, whereas all the following step edges were cut to 45°. The flow impacts in (a) onto the horizontal step face of step 2 resulting in jet deflection and partial nappe flow type beyond step 1. If the first two step edges are

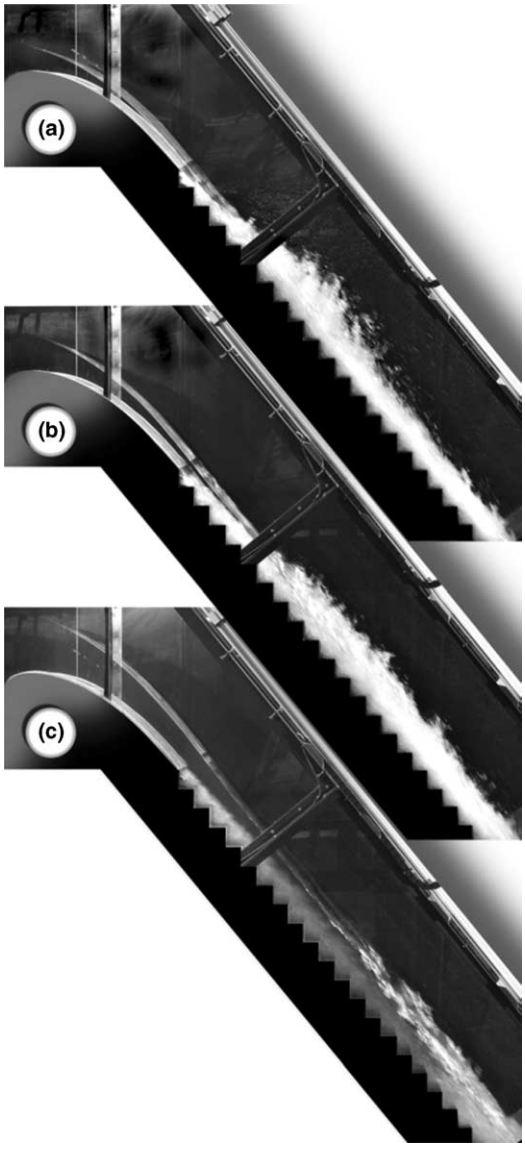

Fig. 8. Stepped chute flow *with* bottom aeration, otherwise as Fig. 7.

cut as previously described, the flow is deflected on the horizontal face of step 3 with a significantly reduced amount of spray. If the first five steps edges are cut, then the flow adheres essentially to the stepped chute and the skimming flow pattern is maintained.

The experimental program involved a total of four specific discharges q_w as shown in Table 2, combined with the three step arrangements (a)–(c) previously referred to. The flows were photographed under identical light conditions and a shutter speed of 0.50 s. The resulting pictures were treated with photo imagery to define the approximate limit between air–water flow, and spray. Fig. 11 shows the relative spray (subscript s) height h_s/s as a function of the relative distance x/s with s as the step height. The maximum spray height so determined was found to correspond approximately to h_{98}, i.e. a flow depth where the air concentration is 98%. It increases both as the discharge and the number of cut steps reduces. The origin of spray formation is always the step downstream of the last 'treated step edge'. The virtual origin of spray flow is $x_0 = (n+1)s/\sin\phi$, therefore, with n as the number of cut step edges.

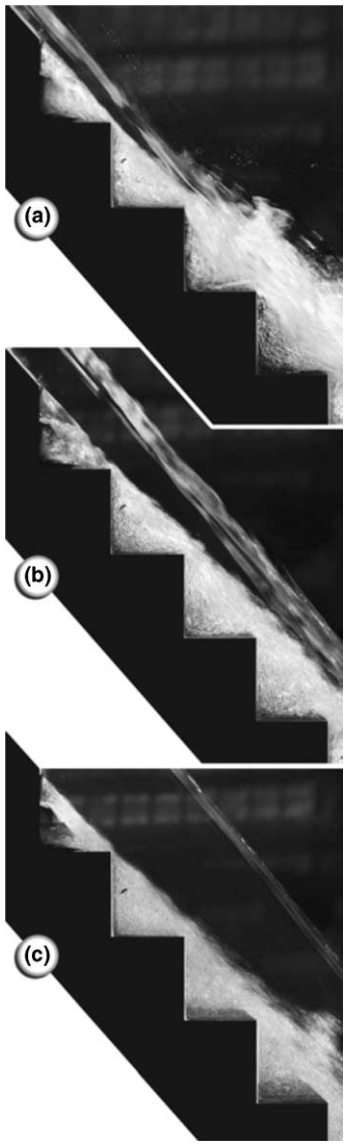

Fig. 9. Details of air entrainment for cases (a)–(c) from Table 1.

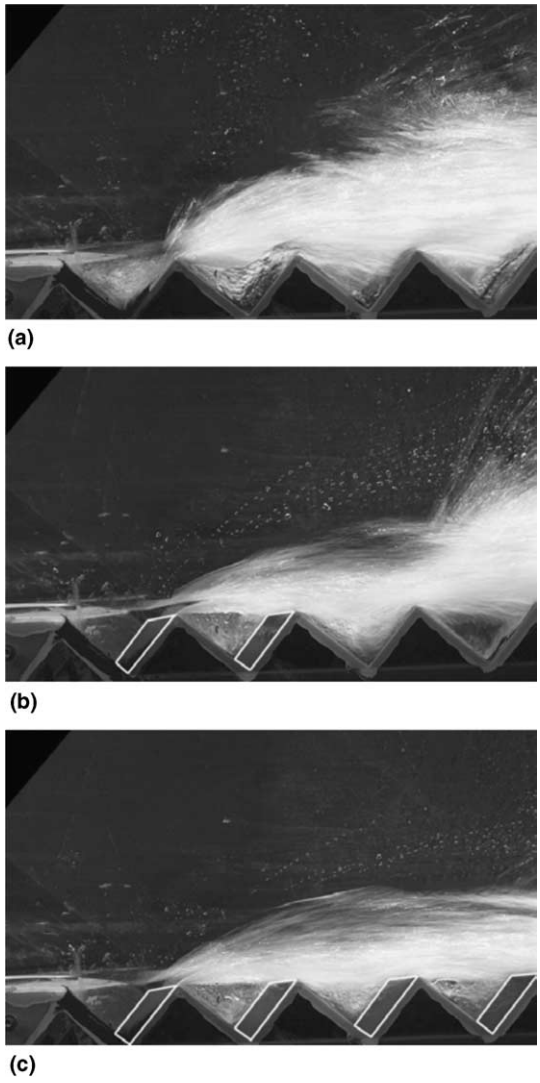

Fig. 10. Flow pattern over stepped chute ($x/s < 5.3$) with different step edge arrangements for $n =$ (a) 0, (b) 2, (c) 5 and $h_c = 0.055$ m.

Table 2
Test data for spray reduction

h_c [m]	q_w [m^2/s]	h_o [m]	F_o [–]
0.034	0.020	0.006	12.8
0.055	0.040	0.012	9.2
0.087	0.080	0.024	6.9
0.138	0.160	0.046	5.2

The data collected were further treated by using the normalized parameters $Y_s = (h_s - h_o)/(h_{s,max} - h_o)$ in which $h_{s,max}$ is the absolute maximum spray elevation for a certain test and $X_s = (x - x_o)/(sF_o)$. The multiplication by $(1/F_o)$ of the 'transverse' coordinate is a standard procedure in supercritical flow, and corresponds to the Mach angle in supersonic flows. Fig. 12(a) shows the transformed spray profiles $Y_s(X_s)$ with a trend line for the rising limb expressed with $R^2 = 0.95$ as

$$Y_s = [1.3 \cdot X_s \cdot \exp(1 - 1.3 \cdot X_s)]^{1/2}, \quad \text{for } 0 < X_s < 1.5 \tag{7}$$

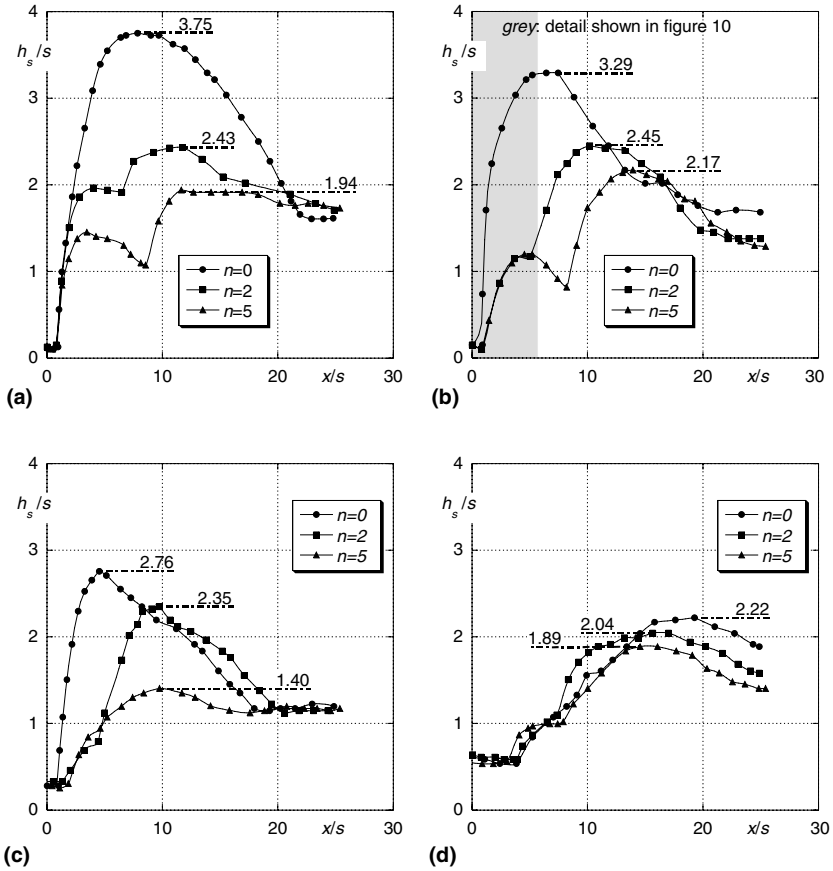

Fig. 11. Relative spray elevation profiles h_s/s versus normalized streamwise coordinate x/s for h_c [m] = (a) 0.034, (b) 0.055, (c) 0.087 and (d) 0.138 and $n = 0$, 2 and 5 treated step edges.

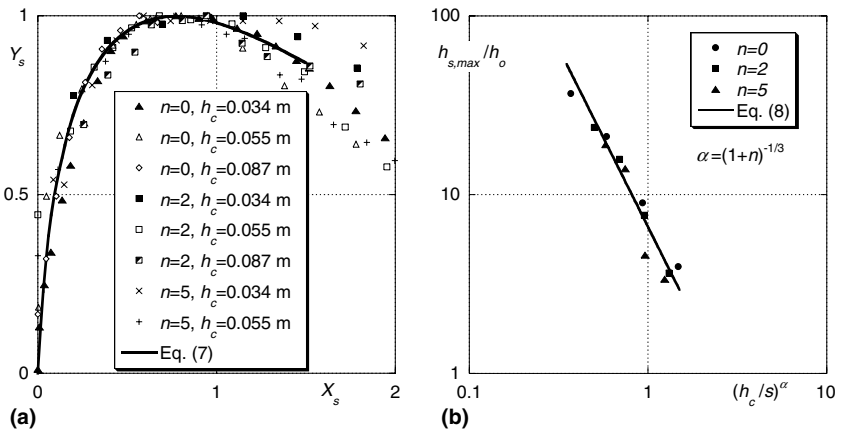

Fig. 12. (a) General spray profile $Y_s(X_s)$ with (—) (7), (b) maximum relative spray elevation $h_{s,max}/h_o$ as a function of relative discharge $(h_c/s)^\alpha$ with (—) (8).

The maximum spray height relative to the flow depth h_o upstream of the first step (Fig. 1) was correlated to the relative critical flow depth h_c/s. Fig. 12(b) shows the result and the fit with $R^2 = 0.97$ as

$$\frac{h_{s,max}}{h_o} = 6.6\left(\frac{h_c}{s}\right)^{-2\alpha}, \quad \text{for } 0.35 < (h_c/s)^{\alpha} < 1.5 \tag{8}$$

The exponent α was related to the number of cut step edges as $\alpha = (1+n)^{-1/3}$. This plot indicates at once that spray becomes a concern for small relative discharge h_c/s, whereas the effect of the number of treated step edges is relatively small for $n \geqslant 2$. The plot also draws to the fact that spray development is much smaller for stepped chutes with a small step height than for those with a large height. Mateos Iguácel and García's (2000) approach may thus be considered a particular case of the present finding.

5. Conclusions

Two important issues of stepped chute flow were addressed in this research, namely pre-aeration of flow and spray reduction by cut step edges. A simple solution was forwarded to both aspects for a particular stepped chute geometry. Pre-aeration of stepped chutes is important in connection with the increase of discharge per unit width to counter cavitation damage upstream from the air inception point. A step aerator was placed in the first step niche to aerate the bottom chute zone. This aerator provides a thin diffusion air layer along the chute in which air bubbles are present up to the point of incipient aeration from the free surface. The hydraulic characteristics of the air–water flow were analyzed in terms of maximum air concentration, the bottom air concentration distribution, the air layer thickness development in the streamwise direction, the free surface profiles both for the blackwater and the whitewater flows and the energy dissipation along the chute. It was concluded that the aerator proposed adds a small but sufficient amount of air for the improved hydraulic chute performance for a larger design discharge as currently adopted. Further, it was stated that the current design procedure applies also for pre-aerated chute flow because the amount of air supplied is relatively small.

The reduction of spray along a stepped chute was accomplished with improved step geometry close to the chute beginning. Instead of standard steps with a right-angled step edge, the latter were cut to direct the small depth flow onto the sloping instead of horizontal step edges. Three basic arrangements were tested for the VAW stepped chute resulting in a significant spray reduction if the first two step edges are cut. The mechanism of spray formation was described and means to counter were presented. A generalized spray profile was also defined in terms of basic parameters. Therefore, in both existing and novel stepped chutes the current limitations in the hydraulic performance are removed to a great extent.

Acknowledgements

The first author was supported from the Swiss National Science Foundation, Grant 200021-101548/1.

Appendix 1

The cavitation index at the point of bottom air inception (subscript i) along a stepped chute may be predicted using information from Boes and Hager (2003a). For a given unit discharge q_w, the mixture flow depth h_{mi} at the inception point follows form their Eq. (5). Using the average air concentration $C_{ia} = 0.228$ at the inception point results in the blackwater flow depth $h_{wi} = h_{mi}(1 - C_{ia})$ and the corresponding blackwater velocity $v_{wi} = q_w/h_{wi}$. These data allow for the computation of the cavitation index $\sigma_{bi} = (h_{pi} - h_v + h_a)/[v_{wi}^2/2g]$ at the bottom inception point x_i in which h_{pi} is the bottom pressure head, h_v the vapor pressure head and h_a the atmospheric pressure head. Fig. 13 relates the cavitation index σ_{bi} to the prototype unit discharge q_w [m^2/s] for a step height $s = 1.20$ m and $\phi = 50°$. The cavitation index for $q_w = 30$ m^2/s is $\sigma_{bi} = 0.42$, whereas it is $\sigma_{bi} = 0.17$ for $q_w = 100$ m^2/s. Accordingly, the bottom air inception point is the most critical location for cavitation damage: Further upstream from the point $x = x_i$, the cavitation index is larger, whereas the flow close to the chute bottom is aerated further downstream. The critical value of σ_c is significantly higher for stepped chutes than for smooth chutes with $\sigma_c = 0.20$ (Pfister et al., in press). To counter cavitation damage on a stepped chute, an aerator is required upstream from the bottom air inception point for discharges larger than the limit discharge previously referred to.

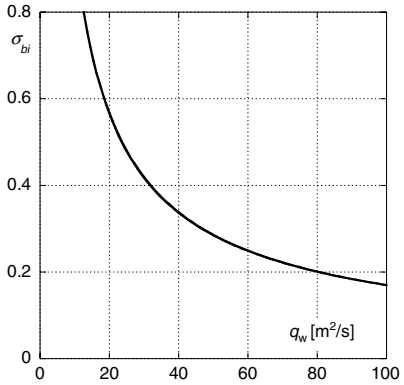

Fig. 13. Cavitation index σ_{bi} at the bottom inception point of a stepped chute as a function of unit discharge q_w [m^2/s] for $s = 1.20$ m and $\phi \cong 50°$.

References

Boes, R.M., 2000. Zweiphasenströmung und Energieumsetzung an Grosskaskaden. Ph.D. Dissertation 13510. Swiss Federal Institute of Technology ETH: Zurich (in German).

Boes, R.M., Hager, W.H., 2003a. Two-phase flow characteristics of stepped spillways. J. Hydraul. Eng. 129, 661–670.

Boes, R.M., Hager, W.H., 2003b. Hydraulic design of stepped spillways. J. Hydraul. Eng. 129, 671–679.

Chamani, M.R., 2000. Air inception in skimming flow regime over stepped spillways. In: Minor, H.-E., Hager, W.H. (Eds.), Hydraulics of Stepped Spillways. Balkema, Rotterdam, pp. 61–67.

Falvey, H.T., 1990. Cavitation in chutes and spillways. Engineering Monograph 42. Bureau of Reclamation, Denver.

Hager, W.H., Blaser, F., 1998. Drawdown curve and incipient aeration for chute flow. Can. J. Civil Eng. 25, 467–473.

Mateos Iguácel, C., García, V.E., 2000. Stepped spillway studies at CEDEX. In: Minor, H.-E., Hager, W.H. (Eds.), Hydraulics of Stepped Spillways. Balkema, Rotterdam, pp. 87–94.

Ohtsu, I., Yasuda, Y., Takahashi, M., 2001. Discussion to onset of skimming flow of stepped spillways, by M.R. Chamani and N. Rajaratnam. J. Hydraul. Eng. 127, 522–524.

Pfister, M., Kramer, K., Minor, H.-E., 2002. Kaskadenbelüfter—Hydraulische Modellversuche. VAW Mitteilung 174. VAW, ETH, Zurich, pp. 417–426 (in German).

Pfister, M., Hager, W.H., Minor, H.-E., in press. Bottom aeration of stepped spillways. J. Hydraul. Eng.

Pinto, N.L. de S., Neidert, S.H., Ota, J.J., 1982. Aeration at high velocity flows. Water Power Dam Constr. 54, 34–38, 54, 42–44.

Rutschmann, P., Hager, W.H., 1990. Air entrainment by spillway aerators. J. Hydraul. Eng. 116, 765–782, 117, 545; 118, 114–117.

Sánchez Juny, M., Pomares, J., Dolz, J., 2000. Pressure field in skimming flow over a stepped spillway. In: Minor, H.-E., Hager, W.H. (Eds.), Hydraulics of Stepped Spillways. Balkema, Rotterdam, pp. 137–145.

Vischer, D.L., Hager, W.H., 1998. Dam Hydraulics. Wiley & Sons, Chichester.

Volkart, P., Chervet, A., 1983. Air slots for flow aeration. VAW Mitteilung 66. VAW, ETH, Zurich.